Simulation of Nucleus-Nucleus Interactions in the Framework of the FRITIOF Model at the Energy of 3.3 GeV/nucleon

A.S. Galoyan [1], A. Polanski [2], V.V. Uzhinskii

Joint Institute for Nuclear Research,
Laboratory of Information Technologies

Abstract

The intranuclear cascade model overestimates the multiplicity of produced mesons in nucleus-nucleus interactions without taking into account meson and baryon resonance production. Inclusion of the resonances leads to decreasing multiplicity of mesons, neutrons and protons. In order to overcome the problem, it is proposed to use the FRITIOF model adapted to low energies in a combination with the reggeon theory inspired model of nuclear destruction. It is shown that the combination allows one to reproduce satisfactory the meson and baryon yields in the nucleus-nucleus collisions at the energy of 3.3 GeV/nucleon. The combined model works faster than typical quantum molecular dynamic model, and allows one to estimate the data needed for creation of electro-nuclear amplifier.

1 Introduction

Data on nuclear reactions at the energies of hundred MeV and GeV are required for multiple purposes such as long-lived radioactive waste transmutation, material analysis, nuclear medicine as well as research of the cosmic ray effects on spaceships and astronauts. Experiments on measuring the data are costly to be carried out and there is a limited number of facilities to make them. Therefore, reliable computer models for a simulation of the reactions are created to provide the necessary data. Most of them are using the ideas of the cascade-evaporation model (CEM) (see [1] - [6]).

The cascading of nucleons and π-mesons was considered only by the first variants of the model. A good description of hadron-nucleus interactions was reached at the studies. The best result was obtained by S. Mashnik [7]. Though, the application of the model for description of nucleus-nucleus collisions has shown that the model gives a satisfactory yield of the nucleon but overestimates the meson production. Taking into account meson and baryon resonances production is one of the possible ways to solve the problem.

A number of authors were trying to do this, and they usually obtained a decreasing yield of mesons and baryons. It is natural because the effective decreasing of the multiplicity of the produced particles leads to a less powerful cascading. So, a problem of a self consistent description of the meson and baryon yields in hadron-nucleus and nucleus-nucleus interactions appeared.

Let us note that the nuclear destruction mechanism and the procedure of the excitation energy calculation were not changed in the mentioned approaches. Maybe, they led to

[1]Yerevan Physical Institute and Joint Institute for Nuclear Research, e-mail: galoyan@cv.jinr.ru
[2]Soltan Institute for Nuclear Studies, 05-400 Swierk, Poland, e-mail: polanski@cv.jinr.ru

the unsatisfactory results. In this paper we consider a synthesis of the FRITIOF model [8, 9] which takes into account the resonances production and the reggeon theory inspired model of the nuclear destruction [10, 11].

The FRITIOF code [9], that is a program of Monte Carlo simulation of the inelastic hadron-hadron, hadron-nucleus and nucleus-nucleus interactions, is very popular in high energy experimental physics. It is explained by its access, its physical ideas simplicity and a defined beauty of the code by itself. It is easy to use.

The FRITIOF model [8, 9] assumes that an excitation of hadrons into continuum mass spectra takes place in the inelastic hadron-hadron collisions. In the case of the hadron-nucleus or the nucleus-nucleus interactions the excited hadrons can suffer an additional collisions with the nuclear nucleons and go into more excited states, or de-excite. The excited hadrons are considered as quark strings, and the corresponding quark model [12, 13] is used for description of their decay. The probabilities of the multiple collisions are calculated within the Glauber model [14] – [19]. The inelastic collisions are usually considered only [19]. In order to reproduce the baryon yield, we introduce elastic re-scattering too.

It is assumed that the program can not be used at the relatively low energies as the hypothesis about the creation and decay of the quark strings is not valid. Attempts of compelling the program to operate at the energies below 5-10 GeV/nucleon for AA-interactions usually failed. Though the analysis of the code operation shows that the program cycles due to its quite simple-hearted interpretation of the Fermi-motion of the nucleons. A change of the Fermi-motion simulation algorithm [20] allowed one to decrease a formal limit of the model application region.

Now in order to use the model at the intermediate energies, one needs to correct a scheme of the fragmentation of the quark string with low masses because in this case the excited hadrons have low masses, too. Below the corresponding changes of the model will be presented which allow one to reach a defined success. To solve the problem, we have used the experimental data on the neutron-proton interactions at momentum 1.25 – 5.1 GeV/c [21] given amiable by the Yu. A. Troyan's group of the neutron-proton interaction study.

One of the disadvantages of the FRITIOF code is an omission of the slow particle cascading into the nuclei. Under the "cascading" one usually understands the standard intranuclear cascade scenario (see, e.g., [1]), which neglects the quantum mechanical effects. The quantum mechanical description of the particles cascading in the nuclei can be achieved in the framework of the reggeon theory. According to the reggeon approach [22], a consideration of the cascade interactions necessitates a calculation of the yields of the so-called enhanced diagrams to the elastic scattering amplitude. Using the procedure for the calculation proposed in [23] and Abramovski-Gribov-Kancheli cutting rules [24], one can obtain the positive defined cross-sections of the inelastic processes. At first glance, this returns one to the classical cascade picture of the interactions. However, there is an essential difference. The cascade model assumes that the cascade is developed in a three-dimensional space of a target nucleus. According to the reggeon approach [10], the "cascade" of the reggeon exchanges occurs in a two-dimensional space of projected radius-vectors of nucleons on the plane perpendicular to the momentum of projectile particle (on a plane of impact parameter), with a "cascade power" independent of the multiplicity of the produced particles and defined by the reggeon vertex constants and the size of nucleus. We shell give a corresponding algorithm in Sec. 3. The main calculation results

are presented in Sec. 4. We are starting with a short description of the main assumptions of the FRITIOF model.

2 Theses of the FRITIOF model

The FRITIOF model assumes that the hadron-hadron interactions are of two-particle character

$$a + b \longrightarrow a' + b', \tag{1}$$

where a' and b' are a and b hadrons in excited states. The kinematics of the reaction is determined as follows: in the center of mass of colliding hadrons the energy-momentum conservation low has the form:

$$\begin{aligned} E_a + E_b &= E_{a'} + E_{b'} = \sqrt{s_{ab}}, \\ p_{az} + p_{bz} &= p_{a'z} + p_{b'z} = 0, \\ 0 &= \vec{p}_{a'\perp} + \vec{p}_{b'\perp}, \end{aligned} \tag{2}$$

where E_a and E_b ($E_{a'}, E_{b'}$)- energies of the initial (final) hadron a and b (a', b'), p_{az} and p_{bz} - longitudinal momentum components (projected momenta on the interaction axis).

Adding and subtracting the first two equations from (2), we get

$$\begin{aligned} P_a^+ + P_b^+ &= P_{a'}^+ + P_{b'}^+ \\ P_a^- + P_b^- &= P_{a'}^- + P_{b'}^- \\ 0 &= \vec{p}_{a'\perp} + \vec{p}_{b'\perp}, \end{aligned} \tag{3}$$

where $P^+ = E + p_z, \quad P^- = E - p_z$.

At high energies: $P_{a'}^- \simeq m_{a'}^2/2 \mid p_{a'z} \mid, \quad P_{b'}^+ \simeq m_{b'}^2/2 \mid p_{b'z} \mid$. Thus, the $P_{a'}^-$ and $P_{b'}^+$ distributions used in the code have the form

$$\begin{aligned} dW &\sim dP_{a'}^-/P_{a'}^- \simeq dm_{a'}^2/m_{a'}^2, \\ dW &\sim dP_{b'}^+/P_{b'}^+ \simeq dm_{b'}^2/m_{b'}^2. \end{aligned} \tag{4}$$

The limits of $P_{a'}^-$ and $P_{b'}^+$ are defined as

$$[P_a^-, P_b^-], \quad [P_b^+, P_a^+]. \tag{5}$$

The distributions (4) are typical for the so-called high-mass diffraction dissociation processes.

Knowing $P_{a'}^-$, $P_{b'}^+$, $\vec{p}_{a'\perp}$, $\vec{p}_{b'\perp}$ and determining $P_{a'}^+$, $P_{b'}^-$ from Eqs. (3), one can find the masses of the excited hadrons a' and b'. $\vec{p}_{a'\perp}$ and $\vec{p}_{b'\perp}$ are sampled according to the low

$$dW \sim exp(-\vec{p}_{a'\perp}^2/ < p_\perp^2 >)\ d^2p_{a'\perp}. \tag{6}$$

In case of hadron-nucleons interactions the kinematics governed by Eqs. (3), (4), (6) is applied to the first collision of the projectile nucleon with one of the target nucleons ($a + N_1 \rightarrow a' + N_1'$). For the second collision ($a' + N_2 \rightarrow a'' + N_2'$), analogous relations are used, but (5) is replaced for

$$[P_{a'}^-, P_{N_2}^-], \quad [P_{N_2}^+, P_{a'}^+]. \tag{7}$$

As a result, the consequent collisions involve a systematic increasing of the mass of hadron a if transfers of the transverse momentum are small.

A similar approach is also applied to simulate the nucleus-nucleus interactions. Here the reactions $a' + b' \to a'' + b''$ are considered. The above distributions on $P^-_{a'}$ and $P^+_{b'}$ are replaced by those on $P^-_{a''}$ and $P^+_{b''}$ and the limits of $P^-_{a''}$ and $P^+_{b''}$ are redefined as

$$[P^-_{a'}, P^-_{b'}], \quad [P^+_{b'}, P^+_{a'}]. \tag{8}$$

At relatively lower energies of the order of 5–10 GeV/nucleon, the FRITIOF model without taking into account hadron de-excitation overestimates the multiplicity of the produced particles in hA- and AA-interactions. To this end we have changed the condition (8) by the following giving an allowance for considering the excitation process with the increasing mass and the de-excitation process with decreasing mass:

$$[P^-_a, \sqrt{s_{a'b'}} - m_b], \quad [P^+_b, \sqrt{s_{a'b'}} - m_a]. \tag{9}$$

P^-_a and P^+_b are calculated at $s_{ab} = s_{a'b'}$, $m_{a'} = m_a$, $m_{b'} = m_b$. The minimal values of P^-_a and P^+_b, being the lower limits in (9), are obviously reached in the reaction $a' + b' \to a + b$. The maximal values are achieved at $p_{a''z} = p_{b''z} = 0$ when hadrons come to rest in the c. m. frame of NN-collision.

The reactions (1), or

$$a + b \longrightarrow a' + b, \tag{10}$$

$$a + b \longrightarrow a + b', \tag{11}$$

are the so-called diffraction dissociation reactions. The reactions (10), (11) are one-vertex diffractions, the reaction (1) is a double vertex diffraction. It is obvious that a minimal mass of the excited nucleon in NN-interactions can be equal to $m_{a'} = m_N + N_\pi = 1080$ MeV. In the FRITIOF model the minimal mass is equal to 1.2 GeV. Due to this, the one vertex diffraction with excitation only one hadron is possible at $\sqrt{s_{NN}} \leq 2.4$ GeV, or at $P_{lab} \leq 1.91$ GeV/c in NN-interactions. There can be a two vertex diffraction at higher energies. A relation between the cross-sections of the processes is determined by the hadrons a' and b' mass distributions.

The excited hadrons a' and b' are considered as quark strings, and the corresponding quark model is used for the simulation of their decay [12, 13]. It is assumed that the quark model can be used at sufficient large string masses what can be created at high energies. Thus the FRITIOF model was used mainly at high energies. One can expect that the FRITIOF model predictions fall into a contradiction with experimental data on the processes where the states with low masses can appear. In order to study the situation, we turn to the data on π^--meson and proton distributions in np-interactions at $P_n = 1.25$–5.1 GeV/c [21].

Fig. 1 shows the experimental and calculated π^--meson rapidity distributions, $y = \frac{1}{2}\ln(E+P_z)/(E-P_z)$, where E and P_z are laboratory energy and longitudinal momentum of π^--meson, respectively. As seen, the distributions calculated according to the original code (dashed lines) are of two-bump structure more pronounced at low energies. It seems like it is a circumstance of the assumed diffractive character of the interactions: the bump at large rapidities is caused by a projectile hadron diffraction, the bump at low rapidities is connected with a target nucleon diffraction. Though, at the neutron momentum of

1.25 GeV/c a diffraction system with mass of 1.2 GeV (the minimal mass of excited nucleon assumed by the FRITIOF model) must be in a rest in the center of mass system, and there must not be a subdivision of the fragmentation regions. Thus, we conclude that the two-bump structure of the calculated distributions is not a circumstance of the diffraction dissociation of the hadrons. It only reflects an anysotropy of the low mass string decay. A direct simulation of the decay of the strings with low masses has shown that the bi-module structure is typical for the decay of the strings with masses lower than 1.7 GeV. Two-particle channel is dominating in the decay of such strings. At higher masses the multi-particle channel gets more probable, and the calculated distributions get more regular.

Taking into account the character of the experimental distributions at $P_n = 1.25$, 1.73 GeV/c, it seems reasonable to simulate an isotropic decay of the strings with low masses in the case of the two-particle decay channel. A boundary value of the string mass of 1.7 GeV below of which we have used the proposed procedure, was chosen requiring a good description of the data. As seen in the Fig. 1 (solid curves), this allows us to describe the experimental data quite well.

A more complete situation appears in the description of the π^--meson distributions in transverse momentum, P_T. The original model predicted the average transverse momentum larger than the experimental ones (see the dashed curves in Fig. 2), though we had changed the character of the low mass string decay. Since at $P_n = 1.25$, we simulate an isotropic decay of the excited hadrons, the maximum of the distribution in P_T is determined by mass of the decayed system. Thus, in order to decrease the average transverse momentum, the minimal mass of the excited nucleon state was decreased to the value of 1.1 GeV. This, as seen from Fig. 2, gave a better result at $P_n < 2$ GeV/c. At larger energies one needs to take into account the transverse momentum transferred by the colliding nucleons.

An analysis of proton spectra gives some additional information, and allows one to determinate the model parameters more exactly. For the analysis we have used the data on the following reactions

$$np \longrightarrow pp\pi^-; \tag{12}$$

$$np \longrightarrow pp\pi^-\pi^0; \tag{13}$$

$$np \longrightarrow np\pi^+\pi^-. \tag{14}$$

In the reaction (12) according to the model the diffraction dissociation processes of the projectile particle is a dominant one. In the reaction (13) the two-vertex diffraction processes do the same. At last, in the reaction (14) we have equal yields of the one-vertex and two-vertex diffraction. Thus, the study of the reactions allows one to check the different components of the model.

Fig. 3 gives the experimental and calculated rapidity distributions of the protons. The experimental data are presented by the histograms, the original model calculations - by the dashed curves, and the last calculations - by the solid curves. As seen, there is a two-bump structure of the experimental distributions on the reactions (12). The bump at small rapidities is caused by the saved target protons. The bump at large rapidities is connected with the protons created in the projectile particle diffraction. The distribution of the reaction (13) has no structure. At last, in the reactions (14) there is a dominant production of the protons in the target fragmentation region.

The original model calculations are in agreement with the data on the reaction (14). At the same time, the calculated distribution for the reaction (12) has a bump in the region $y \sim 1.7$ what does not observe at the experiment. For its elimination we introduce a charge exchange between the nucleons in 50 % of the two-vertex diffraction. This allowed us to improve the proton spectra description in part.

Enumeration of the changes made in the FRITIOF code

1. The minimal mass of the excited nucleon decreases from 1.2 GeV to 1.1 GeV;
2. In case of the two-particle decay channel of a string with a mass lower than 1.7 GeV the isotropic decay is simulated in the center of the mass system;
3. The charge exchange between the colliding nucleons is allowed in 50 % of the two-vertex diffraction;
4. The value of the average square of the transverse momentum which transferred between the colliding nucleons increases from 0.08 $(\mathrm{GeV/c})^2$ to 0.15 $(\mathrm{GeV/c})^2$.

3 Simulation of nuclear destruction at the fast stage of interaction.

3.1 Determination of the number of knocked-out nucleons

In the last few years there have been some successful attempts to describe the hadron-hadron elastic scattering at low and intermediate energies (below $1-2\ GeV$) within the quark-gluon approach (see Refs. [25] - [28]). In Ref. [25] -[28] the amplitudes of $\pi\pi-$, $K\pi-$ and $NN-$ scattering were found and an agreement of the theoretical calculations with corresponding experimental data was reached at the assumption that in the elastic hadron scattering one-gluon exchange with the following quark interchange between hadrons takes place (see Fig. 4a). At high energies two-gluon exchange appropriation (Fig.4b) works quite well (see Ref. [29], [30] and [31]). What kind of exchanges can dominate in hadron-nucleus and nucleus-nucleus interactions?

The simplest possible diagrams of the processes with three nucleons are given in Fig. 5. Calculation of their amplitudes according to Refs. [25]-[28] is a serious mathematical problem. It can be simplified if one takes into account an analogy between the quark-gluon diagrams and the reggeon diagrams: the quark diagram of Fig. 4a corresponds to a one-nonvacuum-reggeon exchange diagram; the diagram of Fig. 4b describes the pomeron exchange in the $t-$ channel; the diagram of Fig. 5a is in a correspondence with the enhanced reggeon diagram of the pomeron splitting into two non-vacuum reggeons. The three pomeron diagram (Fig. 5d) represents a more complicated process. It is rather hard to find a correspondence between the reggeon diagrams and the diagrams of Fig. 5b, 5c.

The reggeon parameters and the functional forms of the amplitudes of 3-reggeon processes are well known. The constants of the reggeon interaction vertexes are poor determined. The 3-pomeron vertex constant G_{PPP} is well established ($G_{PPP} = 1.35^{-2}(GeV)^2$, Ref. [23]). There are only old data [32] and the estimations of Ref. [33] on the values of other constants - G_{PRR} and G_{RRR}, which are large. Nevertheless, we believe that the

properties of the reggeon amplitudes must be taken into account in consideration of the nuclear destruction.

It is obvious that the processes like that in Fig. 5d can not dominate in the elastic hadron-nucleus scattering because they are accompanied by production of a high mass diffraction beam of the particles in the intermediate state. Thus, their yields are dumped by a nuclear form-factor. According to the same reason, the yields of the processes like ones in Figs. 5a, 5b can be small, too. If it is not so, one will expect large corrections to Glauber's cross-sections. The practice shows that the corrections to the hadron-nucleus cross-sections must be lower than 5 – 7 %.

The yield of the diagram of Fig. 5c gives a correction to Glauber's one-scattering amplitude. There must be analogous corrections to the other terms of Glauber's series. The sum of the corrections must lead to small effects in the elastic small angle scattering because the corrections are large at small impact parameters. So, they can manifest themselves at large scattering angles. We assume that they have a big influence on the inelastic process characteristics, too.

According to the reggeon theory, a description of the inelastic reactions can be reached in a consideration of the different cuts of the reggeon diagrams. Here the Abramovski - Gribov - Kancheli cutting rules [24] are often used. The corrections to them were discussed in Ref. [22] in the application to the problem of a particle cascading on the nucleus. As was shown in Ref. [22], summation of the yields of enhanced diagrams allows one to describe increasing of the one-particle spectra in the target fragmentation region. At the same time, the authors of Ref. [22] did not take into account the shadowing effects considered in Ref. [34].

Here we have to note that the yields of the diagrams like that shown in Fig. 5c have no shadowing corrections. The yield of the enhanced diagram of Fig. 5a has a form

$$Y_a \sim exp[-(\vec{b}_1 - \vec{b}_2)^2/3r_a^2 - (\vec{b}_1 - \vec{b}_3)^2/3r_a^2 - (\vec{b}_2 - \vec{b}_3)^2/3r_a^2]$$

where $\vec{b}_1, \vec{b}_2$ and $\vec{b}_3$ are the impact coordinates of the nucleons. At the same time, the yield of the diagram of Fig. 5c according to Refs. [25] - [28] is given by

$$Y_c \sim exp[-(\vec{b}_1 - \vec{b}_2)^2/r_c^2]exp[-(\vec{b}_2 - \vec{b}_3)^2/r_c^2].$$

In the limit of $r_a^2, r_c^2 \ll R_A^2$, where R_A is a nucleus radius, the yields coincide. Thus, we can save the results of Ref. [22] considering them as a summation of the yields of the quark-gluon diagrams.

Let us note that neither Y_a, nor Y_c depend on the longitudinal coordinates or on the multiplicity of produced particles. It is the main difference between the "reggeon cascading" and the "usual" cascading.

As well known, the intranuclear cascade model ([1]-[6]) assumes that in a hadron-nucleus collision the secondary particles are produced due to an inelastic interaction of the projectile particle with a target nucleon. The produced particles can interact with other target nucleons. A distribution on distance l between the first interaction and the second one has a form

$$W(l)\ dl \sim \frac{n}{< l >} exp(-\frac{n}{< l >} l),$$

where $< l >= 1/\sigma\rho_A$, σ is a hadron-nucleon cross-section, n is the multiplicity of the produced particles and $\rho_A \simeq 0.15 fm^{-3}$ is the nuclear density. At the same time the

amplitudes or the cross-sections of the processes shown in Fig.5 have no dependence on l or n. Thus, we expect that in the quark-gluon or reggeon approach the "cascade" will be more restricted than in the cascade model. The difference between approaches can lead to the different predictions for the light nuclei destruction (an effect of the limited volume) and for the characteristics of the heavy nuclei interactions (an influence of a large multiplicity of the produced particles).

To show this, we use a simple method to estimate the nuclear destruction in the framework of the quark-gluon approach.

1. As it was said above, the "reggeon cascade" is developed in the space of the impact parameter. Thus, for its description it is needed to determinate a probability to involve a nucleon into the "cascade". It is obvious that the probability depends on a difference of the impact coordinates of the new and the previously involved nucleons. Looking at the yield of the diagram of Fig. 5c, we choose the functional form of the probability as

$$P(\mid \vec{b}_i - \vec{b}_j \mid) = C_{nd} exp(-(\vec{b}_i - \vec{b}_j)^2/r_n d^2). \tag{15}$$

   Here $\vec{b}_i$ and $\vec{b}_j$ are projections of the radiuses of i^{th} and j^{th} nucleons on the impact parameter plane.

2. The "cascade" is initiated by the primary involved, wounded nucleons. If the constant C_{nd} is small, we can use the Glauber theory for their determination.

3. We assume that all the involved and wounded nucleons are ejected from the nucleus.

The "cascade" looks as follows: a projectile particle interacts with some of the intranuclear nucleons. They are called "wounded" nucleons. The wounded nucleons initiate the "cascade". A wounded nucleon can involve a spectator nucleon into the "cascade" with the probability (15). The latter can involve a second nucleon. The second nucleon can involve a third one, and so on.

A Monte Carlo algorithm for estimation of the nuclear destruction in the nucleus-nucleus interactions which corresponds to the model formulation, includes the following steps:

1. The calculation of the impact parameter distribution in the framework of the Glauber theory [19];

2. The sampling of the impact parameter and the nucleon coordinates;

3. The determination of the wounded nucleons (see Ref. [19]);

4. The determination of the spectator nucleons involved in the "cascade" by the wounded nucleons. If the number of the involved nucleons is equal to zero - exit;

5. If the number of the involved nucleons is not equal to zero, a possibility is considered to involve the other spectators nucleons by the involved ones. If the number of the new involved nucleons is equal to zero - exit. In other case - it is needed to repeat the step 5 taking into account only the new involved nucleons.

The first step is performed only once at the given mass numbers of the projectile and target nuclei. The steps 2 – 5 are repeated until the needed statistics is reached. The steps 4, 5 are applied to the nucleons of projectile and target nuclei.

It is suggested that all the newly involved participants and the "wounded" nucleons are knocked-out from the nucleus.

3.2 Fermi-motion of nucleons

To take into account the energy-momentum conservation law by simulating compound system, let us consider a reaction of the compound system $(1,2)$ with hadron h: $(1,2)+h \to 1+2+h$. Neglecting the transverse momenta, a final state of the reaction will be fully characterized by a value of merely one independent kinematical variable. As the variable, let us take

$$x_1^+ = (E_1 + p_1)/(E_1 + E_2 + p_1 + p_2).$$

It is useful to introduce the analogous quantity x_2^+ which satisfies obviously the relation $x_1^+ + x_2^+ = 1$. At given x_1^+ and x_2^+, the rest of the kinematical variables can be determined by the energy-momentum conservation law.

In case of dissociation of two compound systems A and B containing A and B constituents respectively, let us introduce for the i-th constituent of system A

$$x_i^+ = (E_{Ai} + p_{iz})/W_A^+ \quad and \quad \vec{p}_{i\perp},$$

and for the j-th constituent of system B

$$y_j^- = (E_{Bj} - q_{jz})/W_B^- \quad and \quad \vec{q}_{i\perp},$$

where, $E_{A_i}(E_{B_i})$ and $\vec{p}_i(\vec{q}_i)$ are energy and momentum of i-th constituent from A (B),

$$W_A^+ = \sum_{i=1}^{A}(E_{Ai} + p_{iz}), \quad W_B^- = \sum_{i=1}^{B}(E_{Bi} - q_{iz}).$$

One can find W_A^+ and W_B^- using the energy-momentum conservation low at given $\{x_i^+,\ \vec{p}_{i\perp}\}$, $\{y_i^-,\ \vec{q}_{i\perp}\}$, and determine all kinematical variables for all constituents [20].

According to the experimental evidence [35], the average transverse momentum of spectator fragments obeys the parabolic law:

$$< P_\perp^2 >= \frac{A(A-F)}{A} < p_\perp^2 >, \quad \sqrt{< p_\perp^2 >} = 0.07 \ \ GeV/c.$$

To reproduce this result, the values of $\vec{p}_{i\perp}$ for knocked-out nucleons are simulated according to the distribution

$$dW \propto exp(-\vec{p}_{i\perp}^{\,2}/ < p_\perp^2 >) d^2p_{i\perp}, \sqrt{< p_\perp^2 >} = 0.07. \tag{16}$$

The sum of the transverse momenta (with sign "minus") was ascribed for the residual nucleus.

The choice of x_i^+ is carried out by

$$dW \propto exp[-(x_i^+ - 1/A)^2/(d_x/A)^2]dx_i^+, \quad 0 \le x_i^+ < 1, \quad d_x = 0.07. \tag{17}$$

x^+ of the residual nucleus is determined as $1 - \sum x_i^+$.

It was assumed that the knocked-out nucleons changed their characteristics again. The new values of x_i^+ and $p_{i\perp}$ were simulated using the distributions (16) and (17) at $< p_\perp^2 >= 0.385\ (GeV/c)^2$ and $d_x = 0.2$. The results from [36, 37, 38] were used for determination of the fitting parameters.

3.3 Excitation energy of residual nucleus.

The change of the nuclear destruction mechanism requires a change of the nuclear residual excitation energy calculation procedure. In a self-consistent diagram approach one needs to consider the more complete diagrams and describes bound states of the nucleons. The last problem is not solved in the presented quark-gluon approach which allows one only to calculate an repulsive part of the NN-potential. It is expected that a taking into account the terms with high order vertex constant allows one to calculate the attractive part of the potential too. Until this is not made, we are to use a phenomenological approach. Here we follow the Ref. [39].

In paper [39] proton-nucleus interactions at intermediate energies were analyzed. The first stage of the interactions was considered within the Glauber approach. It was assumed that the projectile hadron undergoes successive interactions (elastic and inelastic) with target nucleon. In each of the collisions a part of the energy of the projectile hadron, E, is transferred to the target nucleon. The distribution on the transfer energy was chosen in the form:

$$F_1(E) = \frac{1}{\langle E \rangle} e^{-E/\langle E \rangle}. \tag{18}$$

The authors of Ref. [39] supposed that the excitation energy of residual nucleus was the sum of the recoil nucleon energies. As a result, they described experimental data on neutron multiplicity dependence upon the excitation energy of the residual nuclei.

To apply this approximation to AA-interactions at high energies, one needs to evaluate the number of re-scatterings of each of the knocked-out nucleons. Taking into account that most of AA-interactions are of peripheral nature, we assume that the slow nucleons knocked-out from the peripheral parts of nucleus can not penetrate deeply inside the nucleus because of the large NN cross-section. Their re-scatterings thus occur in the nearest environment. We consider the environment as the spectator nucleons being inside a sphere with radius $r_0 = 2$ fm surrounding a wounded or involved nucleon in its initial state. It is assumed that each spectator nucleon may acquire recoil energy distributed according to Eq. (18). Remember, that the nucleon coordinates were chosen randomly and independent according to the Saxon-Woods distribution. If a spectator nucleon was a neighbor of two "wounded" ones, or involved nucleons, it received the sum of two energies chosen according to Eq. (18), and so on. The sum of energies transferred to all spectator nucleons was considered as the excitation energy of the residual nucleus.

Unlike the CEM, this method obviously will lead to the zero-excitation energy when all nucleons are be ejected.

It also seems evident that the boundary between the spectator part of the nucleus and the part affected by the first stage of the interaction which governs the excitation energy of the residual nucleus, depends on the impact parameter. For example, with heavy projectile nuclei the excitation energy rises with decreasing impact parameter from

$R_A + R_B$ to 0, approaching a maximum and then falls. According to the CEM, it must gradually increase.

We have used $\langle E \rangle = 8$ MeV and the standard evaporation model [40] (see, also Ref. [1]) for simulation of the residual nucleus de-excitation.

4 Description of nucleus-nucleus interactions

Fig. 6 shows the proton and π^--meson rapidity distributions in different nucleus-nucleus interactions. They were calculated by the modified FRITIOF code and by the code of the cascade-evaporation model[3] [41]. Events with at least one inelastic NN-collision were selected at the simulations. As seen, for *dd*-interactions the models give close results. Since in this case we can neglect the cascade interactions, the coincidence of the results tells us about correctness of the NN-interactions description in the CEM (the CEM code used by us does not allow a direct simulation of NN-interactions). We can mark only a little enhanced baryon production in the central rapidity region in the CEM.

In $\alpha\alpha$-interactions where the influence of the cascade interactions is sufficiently large, we observe a difference of the predicted π^--meson spectra. As expected, taking into account the resonances in the FRITIOF model leads to a decreased meson yield. The enhanced meson production in CEM becomes more pronounced in CC-interactions.

To describe the proton production in the nuclear fragmentation regions in the framework of the FRITIOF model, we take into account both inelastic interactions of the nucleons considered above and elastic re-scatterings. As seen, we reproduce the baryon yields in the fragmentation regions at $y \sim 0,\ \ 2.2$ for the *dd*- and $\alpha\alpha$-interactions. The CEM calculations for CC-collisions were used for determination of the nuclear destruction model parameters, $C_{nd} = 1, \quad r^2_{nd} = 1.4$ (fm^2). Then we introduced the experimental criteria for the proton registration.

The calculations for heavy nuclei look most interesting. In Fig. 7 the proton distributions are presented on total and transverse momentum in $n + Ta$ interactions at $P_n = \ 4.2$ GeV/c. As seen, the model predictions are close to each other. The same closeness we observe for $C + Ta$ interactions at $P = \ 4.2$ GeV/c/nucleon presented in Fig. 8. Though, there is a wide difference between the predicted meson spectra. The FRITIOF model calculations are close to the experimental data. At the calculation we use the following values of the parameters $C_{nd} = 0.2, \quad r^2_{nd} = 1.1$ (fm^2) to reproduce the Ta nuclei destruction.

Summing up, we can conclude that we have reached a satisfactory description of the meson and nucleon production in the nucleus-nucleus interactions at the energy of 3.3 GeV/nucleon in the framework of the sufficiently simple FRITIOF model. The model can be applied for practical calculation of nucleus-nucleus interaction characteristics.

The authors of the paper are thankful to Prof. V.S. Barashenkov, Zh.Zh. Musulmanbekov and B.F. Kostenko for useful discussions. One of the authors (V.V.U.) thanks RFBR (grand No. 00-01-00307) for its financial support.

[3)] The model takes into account the trailing effect, Pauli principle, the dependence of the Fermi momentum on the local nuclear density, the pre-equilibrium emission and the evaporation of the nuclei.

References

[1] V.S. Barashenkov and V.D. Toneev// "Interaction of high energy particles and atomic nuclei with nuclei", Moscow, Atomizadt, 1972.

[2] N.W. Bertini et al.// Phys. Rev.,1974, V. **C9**, P. 522.

[3] N.W. Bertini et al.// Phys. Rev., 1976, V. **C14**, P. 590.

[4] J.P. Bondorf et al.// Phys. Lett., 1976, V. **65B**, P. 217.

[5] J.P. Bondorf et al.// Zeit. für Phys., 1976, V. **A279**, P. 385.

[6] V.D. Toneev and K.K. Gudima// Nucl. Phys., 1983, V. **A400**, P. 173.

[7] S.G. Mashnik// "Proceedings of a Specialists Meeting - Intermediate Energy Nuclear Data: Models and Codes". Paris, 1994, P.107.

[8] B. Andersson et al.// Nucl. Phys., 1987, V. **281B**, P. 289.

[9] B. Nilsson-Almquist and E. Stenlund// Comp. Phys. Comm., 1987, V. **43**, P. 387.

[10] Kh.El-Waged, V.V.Uzhinskii// Yad. Fiz., 1997, V. **60**, P. 925.

[11] V.V.Uzhinskii, Kh.Abdel-Waged, A.S.Pak, A.Polanski// JINR Commun., 1995, E2-95-296, Dubna.

[12] T. Sjőstrand// Comp. Phys. Comm., 1986, V. **39**, P. 347.

[13] T. Sjőstrand and M. Bengtsson// Comp. Phys. Comm., 1987, V. **43**, P. 367.

[14] R.J. Glauber// "Lectures in Theoretical Physics", Ed. W.E.Brittin et al., V. **1**, Interscience Publishers, N.Y., 1959.

[15] R.J. Glauber// Proc. of the 2nd Int. Conf. on High Energy Physics and Nuclear structure, (Rehovoth, 1967) Ed. G.A.Alexander, North-Holland, Amsterdam, 1967.

[16] V. Franco// Phys. Rev., 1968, V. **175**, P. 1376.

[17] W. Czyz and L.C. Maximon// Ann. of Phys. (N.Y.), 1969, V. **52**, P. 59.

[18] A. Bialas et al.// Nucl. Phys., 1976, V. **B111**, P. 461.

[19] S.Yu. Shmakov, V.V. Uzhinski, A.M. Zadorojny// Comp. Phys. Commun., 1989, V. **54**, P. 125.

[20] M.I. Adamovich et al. (EMU-01 Collaboration)// Zeit. für Phys., 1997, V. **A358**, P. 337.

[21] A. Abdivaliev et al.//JINR Commun., 1982, **1-82-507**, Dubna.

[22] K.G. Boreskov, A.B. Kaidalov, S.T. Kiselev and N.Ya. Smorodinskaya// Yad. Fiz, 1990, V. **53**, P. 569; Sov. J. Nucl. Phys., 1990, V. **53**.

[23] A.B. Kaidalov, L.A. Ponomarev, K.A. Ter-Martirosyan// Yad. Fiz., 1986, V. **44**, P. 722; Sov. J. Nucl. Phys., 1986, V. **44**.

[24] V.A. Abramovski, V.N. Gribov, O.V. Kancheli// Yad. Fiz., 1973, V. **18**, P. 595; Sov. J. Nucl. Phys., 1974, V. **18**, P. 308.

[25] T. Barnes and E.S. Swanson// Phys. Rev., 1992, V. **D46**, P. 131.

[26] T. Barnes, E.S. Swanson, J. Weinstein// Phys. Rev., 1992, V. **D46**, P. 4868.

[27] T. Barnes, S. Capstick, M.D. Kovarik and E.S. Swanson// Phys. Rev., 1993, V. **C48**, P. 539.

[28] T. Barnes and E.S. Swanson// Phys. Rev., 1992, V. **C49**, P. 1166.

[29] F. Low// Phys. Rev., 1975, V. **D12**, P. 163.

[30] S. Nussinov// Phys. Rev., 1976, V. **D14**, P. 246.

[31] J. Gunion, D. Shoper// Phys. Rev., 1977, V. **D15**, P. 2617.

[32] Yu. M. Kazarinov, B.Z. Kopeliovich, L.I. Lapidus, I.K. Potashnikova// JETP, 1976, V. **70**, P. 1152.

[33] P.E. Volkovitsky// Yad. Fiz., 1988, V. **47**, P. 512; Sov. J. Nucl. Phys., 1988, V. **47**.

[34] R. Jengo, D. Treliani// Nucl. Phys., 1976, V. **117B**, P. 433.

[35] A.I. Bondarenko, V.V. Rusakova, J.A. Salomov, G.M. Chernov// Yad. Fiz., 1992, V. **55**, P. 135; Sov. J. Nucl. Phys., 1992, V. **55**.

[36] D. Armutlisky et al.// Zeit. für Phys., 1987, V. **A328**, P. 455.

[37] H.N. Agakishiev et al.// Yad. Fiz., 1993, V. **56** P. 170; Sov. J. Nucl. Phys., 1993, V. **56**.

[38] A.A. Baldin// Yad. Fiz., 1993, V. **56**, P. 174; Sov. J. Nucl. Phys., 1993, V. **56**.

[39] A.Y. Abul-Magd, W.A. Friedman, J. Hufner// Phys. Rev., 1986, V. **C34**, P. 113.

[40] V. Weisskopf// Phys. Rev., 1937, V. **52**, P. 295.

[41] V.S. Barashenkov, F.G. Zheregy, Zh. Zh. Musulmanbekov// Preprint JINR, 1983, P2-83-117, Dubna.

[42] Ts. Baatar et al.// JINR preprint, P1-99-45, 1999, Dubna (will be published in Yad. Fiz.).

[43] R.N. Bekmirzaev et al.// Yad. Fiz., 1989, **49**, P. 488.

[44] R.N. Bekmirzaev et al.// Yad. Fiz., 1995, **58**, P. 1822.

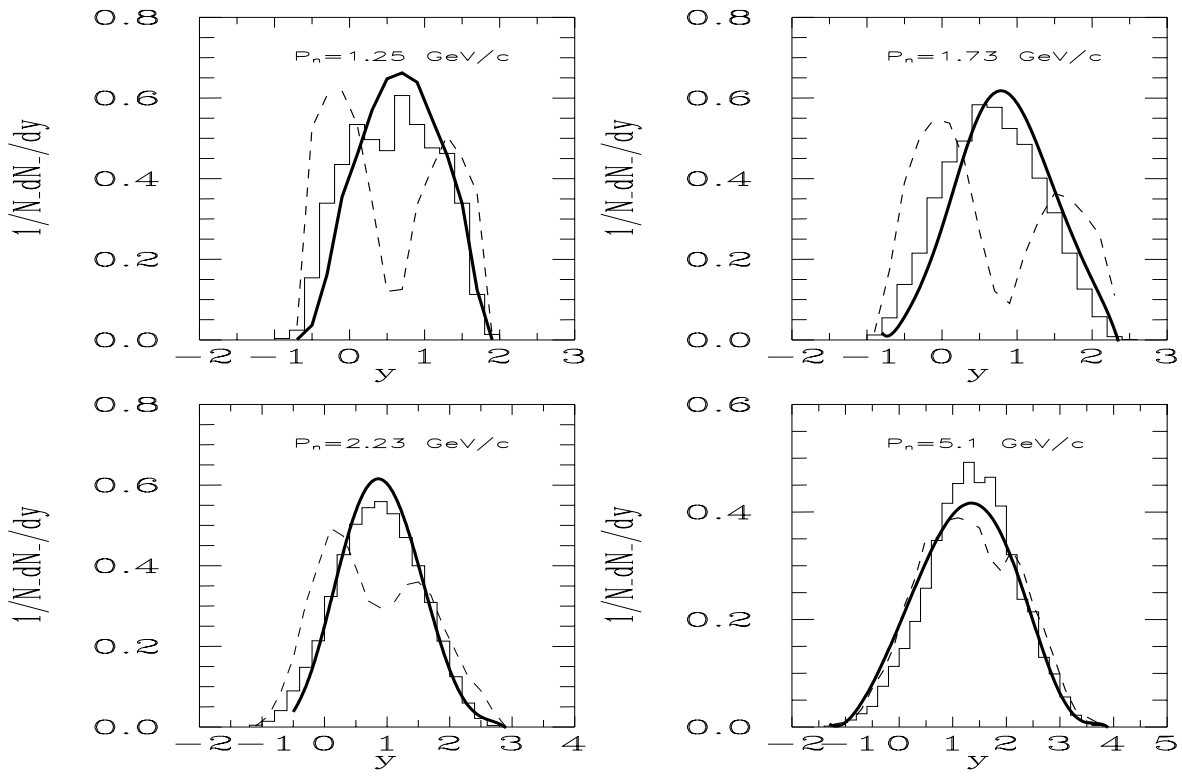

Figure 1: π^--meson rapidity distributions in np-interactions. Histograms are the experimental data. The dashed and solid curves are the standard and modified FRITIOF calculations, respectively.

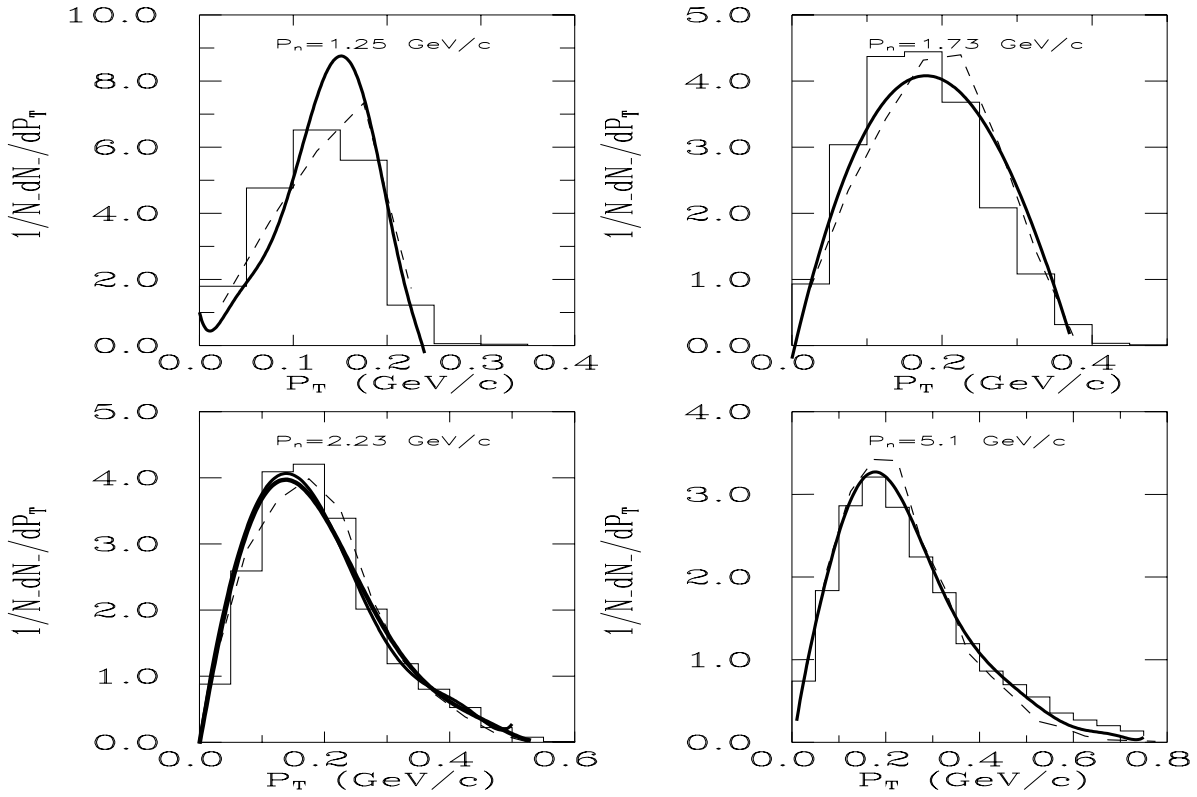

Figure 2: π^--meson transverse momentum distributions in np-interactions. Notations are the same as for Fig. 1.

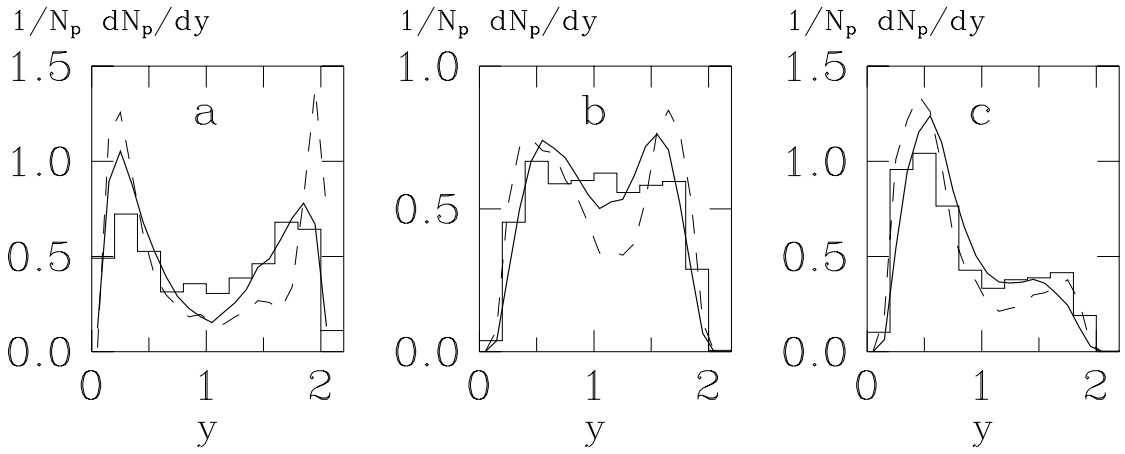

Figure 3: Proton rapidity distributions in a) $np \longrightarrow pp\pi^-$, b) $np \longrightarrow pp\pi^-\pi^0$, c) $np \longrightarrow np\pi^+\pi^-$ reactions at $P_n = 3.83$ GeV/c. Histograms are the experimental data. The solid and dashed curves are the standard and modified FRITIOF calculations, respectively.

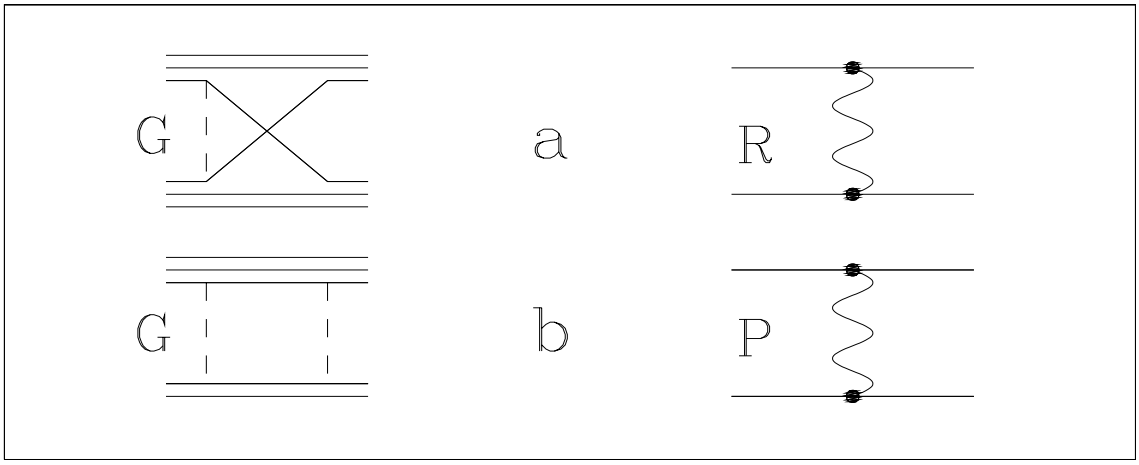

Figure 4:

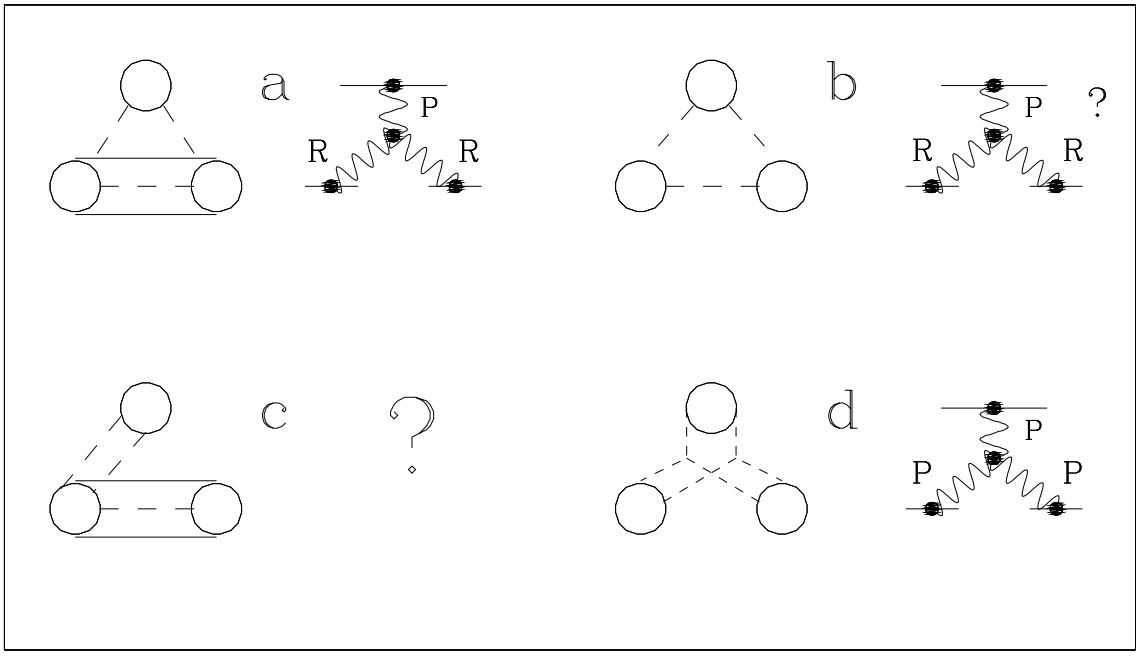

Figure 5:

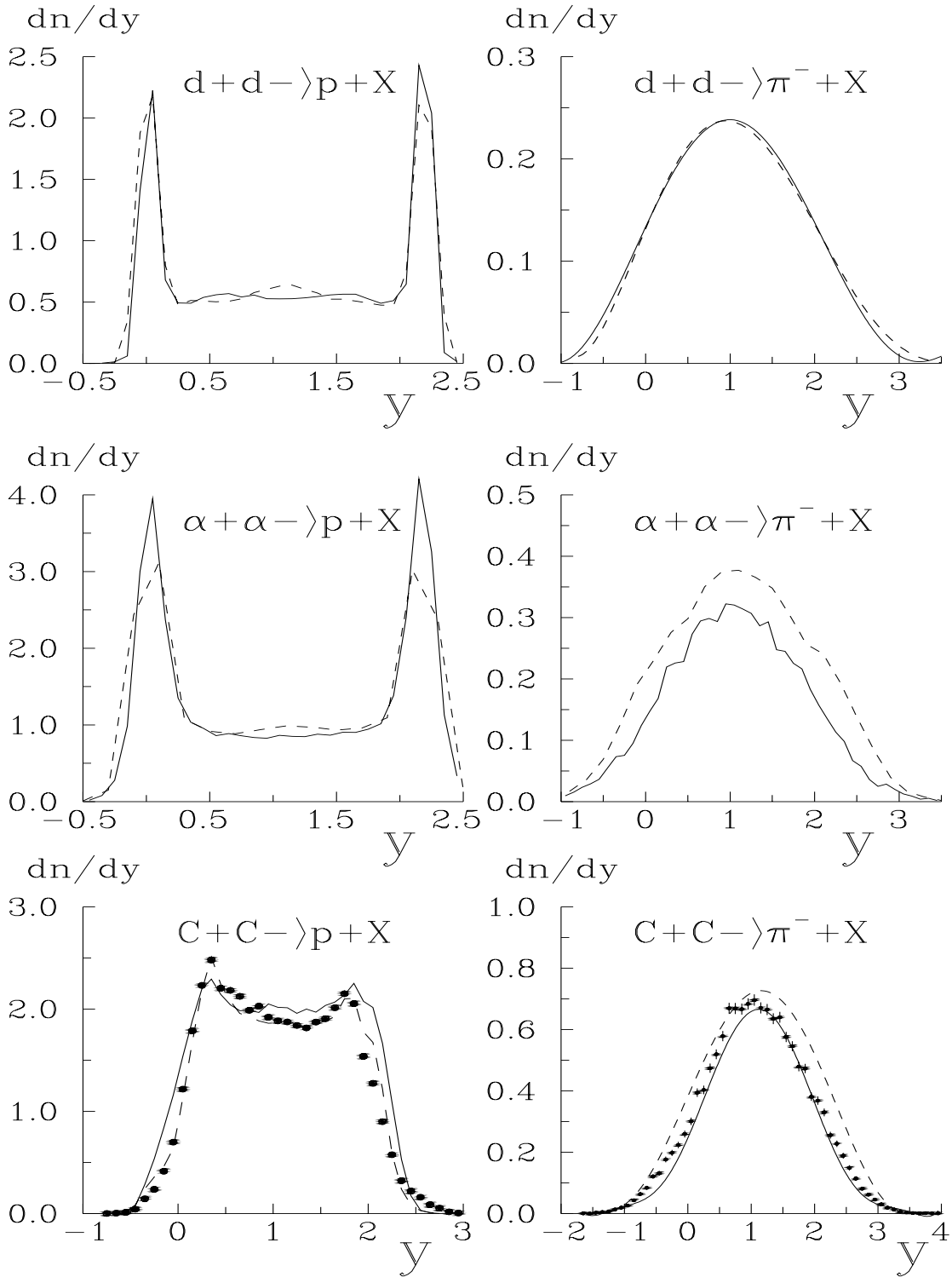

Figure 6: Proton and π^--meson rapidity distributions in nucleus-nucleus interactions at the energy of 3.3 GeV/nucleon. Points are the experimental data Propan The solid and dashed curves are CEM and the modified FRITIOF calculations, respectively.

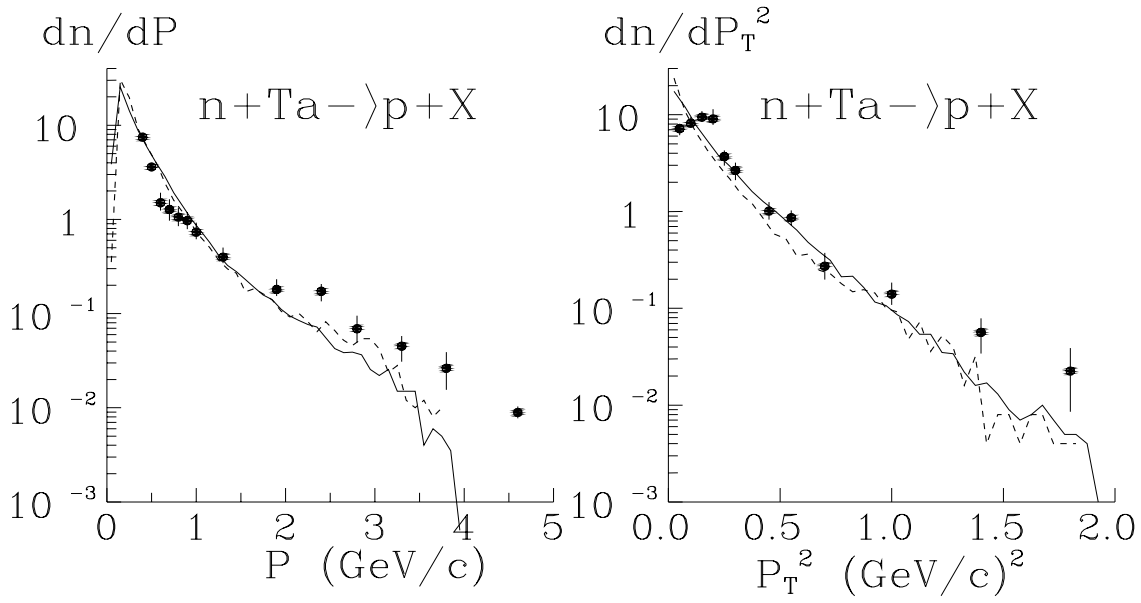

Figure 7: Proton rapidity distributions in nTa interactions. Points are the experimental data [43]. The solid and dashed curves are CEM and the modified FRITIOF calculations, respectively.

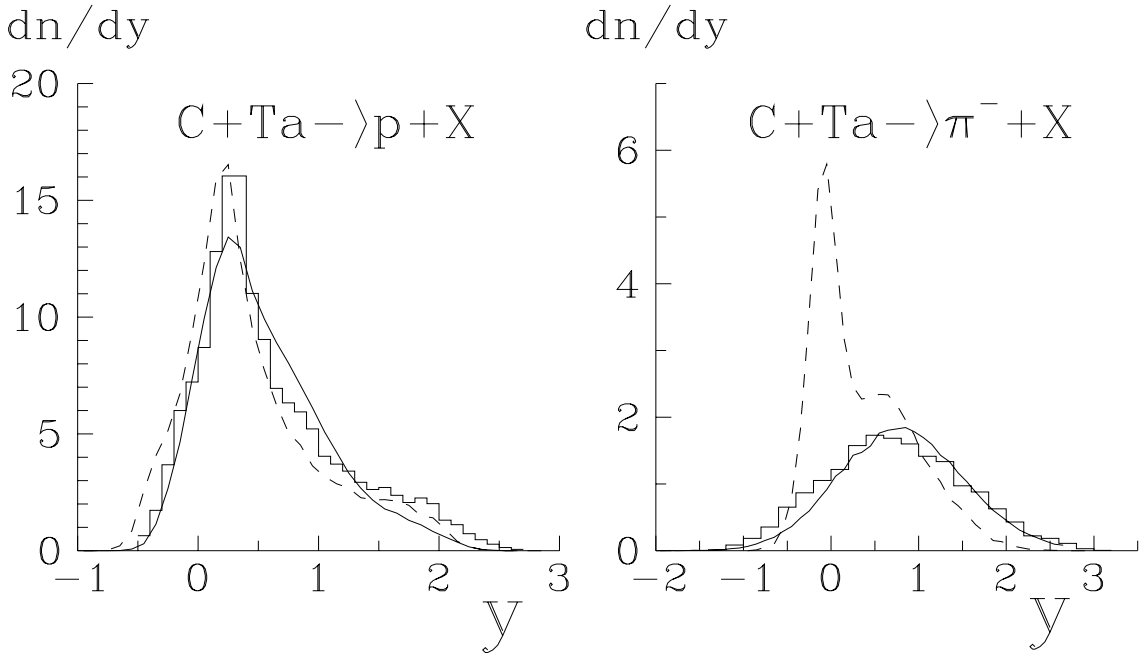

Figure 8: Proton and π^--meson rapidity distributions in CTa-interactions. Points are the experimental data [44]. The solid and dashed curves are CEM and the modified FRITIOF calculations, respectively.